Anal. Chem. **1996,** *68,* 2331−2339

Collision-Induced Dissociation of Branched Oligosaccharide Ions with Analysis and Calculation of Relative Dissociation Thresholds

Sharron G. Penn, Mark T. Cancilla, and Carlito B. Lebrilla*

Department of Chemistry, University of California, Davis, California 95616

Collision-induced dissociation (CID) is used in an external source Fourier transform mass spectrometer (FTMS) equipped with matrix-assisted laser desorption/ionization (MALDI) to study a number of complex, branched oligosaccharides. The relative dissociation thresholds for various oligosaccharide fragmentation pathways have been calculated in terms of kinetic and center-of-mass frame energy. For two isomers of difucosyllacto-*N*-hexaose, the loss of the fucose sugar is always the lowest energy fragment observed and occurs at the same energy for both isomers when the oligosaccharide is coordinated to a sodium ion. When the oligosaccharide is complexed to cesium, the threshold for the removal of the fucose moiety increases, indicating that the cesium is involved in a coordination complex that stabilizes the sugar. MS/MS/MS is performed on a sugar, mannose core, which does not readily fragment during MALDI. In all the sugars examined, CID produces additional structural information relative to MALDI/FTMS.

Oligosaccharides play a key role in many biological functions. In glycoproteins, they are covalently linked to proteins through either O-linked or N-linked glycosidic bonds. Whereas other biomolecules such as proteins and nucleotides form linear structures, oligosaccharides are highly branched and form a number of stereoisomers. While this complex structure is utilized in cell−cell interactions for very specific recognition purposes,[1] it makes the analysis very difficult. Unfortunately, until these detailed structures are known, it may not be possible to fully describe the biological function of such oligosaccharides.

While many separation methods exist,[2] these do not give any structural information. Nuclear magnetic resonance (NMR) spectroscopy can give very detailed structural information, but interpretation of the data for complex oligosaccharides is not trivial, and milligram quantities of pure material are often needed for complex two-dimensional experiments.[3] Much of the early mass spectrometric studies of oligosaccharides were carried out using fast atom bombardment (FAB) as the ionization technique, but this is hampered by poor sensitivity and lack of fragmentation.[4−12] Electrospray ionization (ESI) is another ionization technique amenable to oligosaccharides. Reinhold et al. have reported ESI of methylated glycosphingolipids and have successfully carried out collision-induced dissociation (CID).[13] Many acknowledge that matrix-assisted laser desorption/ionization (MALDI) is the ionization method of choice when analyzing oligosaccharides.[14−22] MALDI is conventionally coupled to time-of-flight (TOF) instruments, but this combination is unable to give detailed structural information. Recently, the advent of postsource decay (PSD) techniques has allowed structural information to be obtained.[23] Spengler et al. have demonstrated the analysis of oligosaccharides using PSD.[24]

In this paper, we present what we believe to be the first report of the CID of MALDI-generated oligosaccharide ions by external source Fourier transform mass spectrometry (FTMS). The advantage of FTMS is that the detection delay can be varied from milliseconds to minutes, compared to only the available microsecond time scale for TOF metastable decay in PSD. Thus, FTMS can observe fragmentation that occurs over a 10^6 times longer time scale than in PSD experiments. Therefore, any fragments observed in PSD should also appear in FTMS. It should be noted that, in PSD experiments, the source and ionization conditions are chosen to be as harsh as possible to lead to the most

(1) Lowe, J. B. *Carbohydrate recognition in cell−cell interactions*; IRL Press: Oxford, UK, 1994.
(2) Lee, Y. C. *Anal. Biochem.* **1990**, *189*, 151.
(3) Lennarz, W. J.; Hart, G. W. *Guide to techniques in Glycobiology*; Academic Press: San Diego, CA, 1994.
(4) Barber, M.; Bordoli, R. S.; Sedgwick, R. D.; Vickerman, J. C. *J. Chem. Soc., Faraday Trans. 1* **1982**, *78*, 1291.
(5) Carr, S. A.; Reinhold, V. N.; Green, B. N.; Hass, J. R. *Biomed. Mass Spectrom.* **1985**, *12*, 288.
(6) Dell, A. *Adv. Carbohydr. Chem. Biochem.* **1987**, *45*, 19.
(7) Domon, B.; Costello, C. E. *Biochemistry* **1988**, *27*, 1534.
(8) Guevremont, R.; Wright, J. L. C. *Rapid Commun. Mass Spectrom.* **1988**, *2*, 50.
(9) Hofmeister, G. E.; Zhou, Z.; Leary, J. A. *J. Am. Chem. Soc.* **1991**, *113*, 5964.
(10) Zhou, Z.; Ogden, S.; Leary, J. A. *J. Org. Chem.* **1990**, *55*, 5444.
(11) Laine, R. A.; Pamidimukkala, K. M.; French, A. D.; Hall, R. W.; Abbas, S. A.; Jain, R. K.; Matta, K. L. *J. Am. Chem. Soc.* **1988**, *110*, 6931.
(12) Orlando, R.; Bush, C. A.; Fenselau, C. *Biomed. Environ. Mass Spectrom.* **1990**, *19*, 747.
(13) Reinhold, B. B.; Chan, S.-Y.; Chan, S.; Reinhold, V. N. *Org. Mass. Spectrom.* **1994**, *29*, 736.
(14) Stahl, B.; Steup, M.; Karas, M.; Hillenkamp, F. *Anal. Chem.* **1991**, *63*, 1463.
(15) Stahl, B.; Thurl, S.; Zeng, J. R.; Karas, M.; Hillenkamp, F.; Steup, M.; Sawatzi, G. *Anal. Biochem.* **1994**, *223*, 218.
(16) Harvey, D. J.; Rudd, P. M.; Bateman, R. H.; Bordoli, R. S.; Howes, K.; Hoyes, J. B.; Vickers, R. G. *Org. Mass Spectrom.* **1994**, *29*, 753.
(17) Bornsen, K. O.; Mohr, M. D.; Widmer, H. M. *Rapid Commun. Mass Spectrom.* **1995**, *9*, 1031.
(18) Ashton, D. S.; Bedell, C. R.; Cooper, D. J.; Lines, A. C. *Anal. Chim. Acta* **1995**, *306*, 43.
(19) Whittal, R. M.; Palcic, M. M.; Hindgaul, O.; Li, L. *Anal. Chem.* **1995**, *67*, 3509.
(20) Mohr, M. D.; Bornsen, K. O.; Widmer, H. M. *Rapid Commun. Mass Spectrom.* **1995**, *9*, 809.
(21) Juhasz, P.; Biemann, K. *Carbohydr. Res.* **1995**, *270*, 131.
(22) Juhasz, P.; Costello, C. E. *J. Am. Soc. Mass Spectrom.* **1992**, *3*, 785.
(23) Kaufman, R.; Spengler, B.; Lutzenkirchen, F. *Rapid. Commun. Mass Spectrom.* **1993**, *7*, 902.
(24) Spengler, B.; Kirsch, D.; Kaufmann, R.; Lemoine, J. *J. Mass Spectrom.* **1995**, *30*, 782.

S0003-2700(96)00155-2 CCC: $12.00

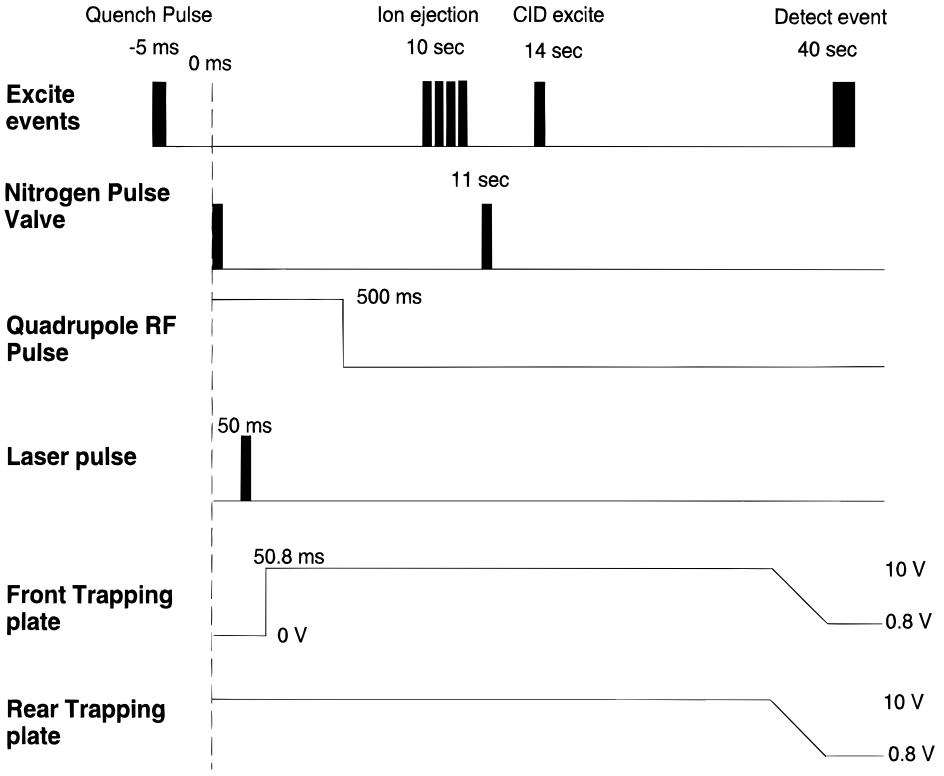

Figure 1. Pulse sequence for CID experiments, not to scale. For description, see Experimental Section.

fragmentation. In the experiments laid out in this paper this has not been necessary. We use a single set of conditions to obtain molecular ions and fragments. A further advantage of FTMS is that CID can be carried out on any fragment ion, and MS^n is relatively straightforward, allowing much more structural information to be obtained.[25]

In this paper, we present MS, MS/MS, and MS/MS/MS results for a number of sodiated and cesiated lactose sugars and mannose N-type sugars, along with a number of dissociation thresholds. These examples illustrate the utility of CID for the analysis and investigation of the fundamental unimolecular dissociation of these important compounds.

EXPERIMENTAL SECTION

Experiments were performed on an external source FTMS, equipped with a 3 T magnet, built in our laboratory and described in detail previously.[26] Data acquisition is performed with an IonSpec data system (IonSpec Corp., Irvine, CA). MALDI is performed using an LSI 337 nm nitrogen laser. The beam is focused on the probe tip, attenuated by one quartz disk, giving a laser irradiance of $\sim 1 \times 10^7$ W/cm^2. An important requirement in MS and MS^n is a pulse valve to allow cooling gas into the ICR cell. This is needed for collisional cooling of the original trapped ions and for collision-induced dissociation. The pulse sequence is important and is shown in Figure 1. A quench pulse 5 ms before the start of the experiment clears the ICR cell of any ions remaining from previous experiments. At 0 ms, the pulse valve is opened for 2 ms, allowing nitrogen to enter the ICR cell (with 18 Torr behind the valve). This pulse collisionally cools the ions sufficiently so they can be trapped, initially, by the 10 V biased front and rear trapping plates, which are lowered to 0.6 V for detection. While the maximum allowed trapping plates voltage is 38 V, 10 V is sufficient for these applications. At 50 ms, the laser fires, producing MALDI ions. McIver et al.[27] have previously shown that, in a MALDI quadrupole FTMS experiment, the relationship between the timing of the laser pulse and the raising of the front trapping plate is important. For the source conditions used for these experiments (quadrupole offset, −10 V; extractor, −303 V), the time between the laser pulse and the raising of the front trapping plate voltage was 0.8 ms. The ions, once trapped, are allowed to cool for 10 s. This ensures they are at the center of the cell before excitation. Following ion cooling, the ejection of the unwanted ions is carried out with a series of sweeps and bursts between 10 and 11 s after the start of the experiment. This isolates the desired ion (usually $[M + Na]^+$) in the ICR cell. It was found that, for ions very close in mass to the ion to be isolated (<20 mass units), it was more beneficial to individually burst each peak (typically 3.5 V for 5 ms) rather than using one sweep over a large mass range. Although this method required the programming of a large number of bursts, we were able to isolate the peak in question with virtually no loss in signal intensity, as can be seen in Figure 2b. At 11 s, the pulse valve is again fired allowing a second burst of nitrogen to enter the ICR cell. At 14 s, the CID burst occurs, at which time the pressure is 3.3×10^{-7} Torr. The best CID results were obtained when a short radio frequency burst (0.25 ms) of high amplitude (17−24 V base-to-peak (V_{b-p}), where base is 0 V) was applied. Larger ions needed higher amplitudes to fragment, as expected. At 40 s, the ions are detected, and the pressure is 7×10^{-8} Torr. This allows the ions to be detected with good resolution and gives sufficient time

(25) Huang, Y.; Pasa-Tolic, L.; Guan, S.; Marshall, A. G. *Anal. Chem.* **1994**, *66*, 4385.

(26) Carroll, J. A.; Penn, S. G.; Fannin, S. T.; Wu, J.; Cancilla, M. T.; Lebrilla, C. B. *Anal. Chem.* **1996**, *68*, 1798.

(27) Li, Y. Z.; McIver, R. T., Jr.; Hunter, R. L. *Anal. Chem.* **1994**, *66*, 2077.

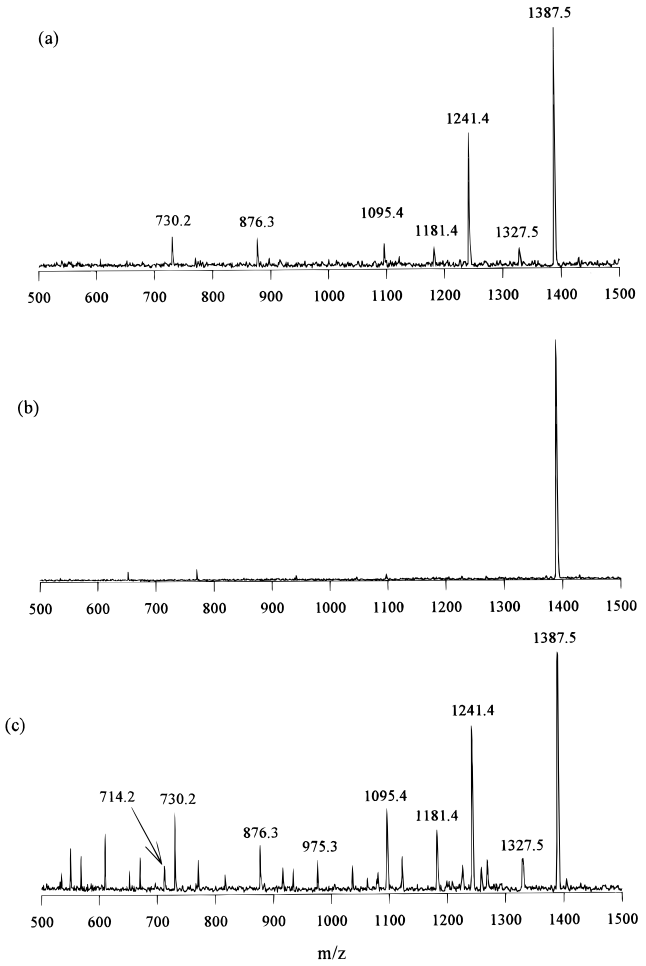

Figure 2. (a) Mass spectrum of difucosyllacto-*N*-hexaose (**I**). (b) Isolation of $[M + Na]^+$ ion of **I**. (c) CID of **I**, excited to 7.22 eV E_{com}.

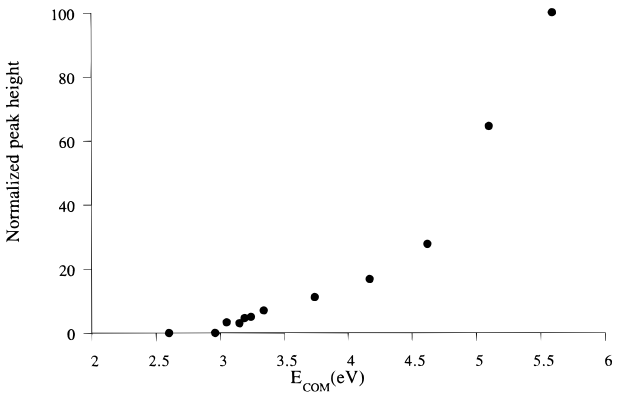

Figure 3. Plot of the appearance of the Y_{3X}'' fragment vs E_{com} for **I**.

for the ions to undergo an "infinite" number of collisions. Between 5 and 10 experiments were summed to give the spectra shown. It should be noted that the pulse valve has since been relocated, so that a pressure of 2.5×10^{-8} Torr is reached within 5 s of the pulse valve firing. This faster rate of pump-down will allow shorter experiment times in the future.

An example of the determination of a dissociation threshold is shown in Figure 3. This shows the normalized peak height of the Y_{3X}'' fragment of oligosaccharide **I** at differing CID voltages. While other groups have developed rigorous methods to accurately determine this threshold for small molecules,[28,29] no methods exist for large and complicated biomolecules. Therefore, we have chosen to select dissociation thresholds simply by monitoring the first occurrence of a fragment. We assign a threshold when a fragment reaches 3% relative intensity. Good signal-to-noise levels are therefore required for this approach. There is a significant source of error in the determination of the dissociation threshold in this manner because, as shown in Figure 3, the onset of threshold may be ambiguous over a 0.5 V_{b-p} range. For Figure 3, the dissociation threshold is determined to be 16.6 V_{b-p}.

CID dissociation thresholds were calculated according to the standard equations,[30]

$$E_{lab} = \frac{q^2 B_0^2 r^2}{2m} \quad (1)$$

where E_{lab} is the laboratory frame energy of the ion (joules), also known as the kinetic energy, m is the mass of the ion (kilograms), q is the charge of the ion (Coulombs), B_0 is the magnetic field strength (Tesla), and r is the cyclotron radius after excitation of the ion (meters). r is obtained from

$$r = \frac{\beta E_0 T_{ex}}{2B_0} \quad (2)$$

where, E_0 is the excitation amplitude (volts peak-to-peak (Vp−p)/m), T_{ex} is the length of the excitation pulse (second), and β is the geometry factor of the cell. The geometry factor for our cell (2 in. × 2 in. × 4 in.) was calculated to be 0.831.[31] Note also that, when we discuss dissociation thresholds in terms of voltages, we are referring to base-to-peak voltages, whereas eq 2 calls for peak-to-peak voltages.

It has been noted in the literature[32] that it is physically more meaningful to discuss collision energies not in laboratory frame energy but in center-of-mass energy. Center-of-mass energy (E_{com}) for one collision can be calculated by

$$E_{com} = \frac{m_t}{m_t + m_p} E_{lab} \quad (3)$$

where m_t is the mass of the target (in our case nitrogen) and m_p the mass of the parent ion. The pulse valve method does not lead to single collision conditions, and thus Freiser and coworkers[33] have suggested, for an "infinite" collision scenario,

$$E_{com\infty} = \frac{m_t + m_p}{m_t + 2m_p} E_{lab} \quad (4)$$

While this equation has been shown to be applicable for the collisions between small aliphatic alcohols and nitrogen, further work is necessary to see if the equation holds true for the larger

(28) Armentrout, P. B.; Halle, L. F.; Beauchamp, J. L. *J. Am. Chem. Soc.* **1981**, *103*, 6501.
(29) Fisher, E. R.; Elkind, J. L.; Clemmer, D. E.; Georgiadis, R.; Loh, S. K.; Aristov, N.; Sunderlin, L. S.; Armentrout, P. B. *J. Chem. Phys.* **1990**, *93*, 2676.
(30) Wood, T. R.; Ross, C. W., III; Marshall, A. G. *J. Am. Soc. Mass Spectrom.* **1994**, *5*, 900.
(31) Grosshans, P. B.; Marshall, A. G. *Anal. Chem.* **1991**, *63*, 2057.
(32) Shukla, A. K. *Rapid. Commun. Mass. Spectrom.* **1990**, *4*, 137.
(33) Burnier, R. C.; Cody, R. B.; Freiser, B. S. *J. Am. Chem. Soc.* **1982**, *104*, 7436.

ions presented in this paper, where the right side of eq 4 approximates to $^1/_2E_{lab}$. Therefore, we present the data for E_{lab} and E_{com} only.

The oligosaccharides studied were two structural isomers of difucosyllacto-*N*-hexaose (**I** and **II**), lacto-*N*-hexaose (**III**), oligomannose 6 (**IV**), and mannose core (**V**), as shown in Chart 1. The lactose-type sugars were obtained from BioCarb Chemicals (Lund, Sweden) and were used without further purification. These sugars were dissolved in methanol at 1 mg/mL. The mannose sugars were obtained from Oxford Glycosystems (Oxford, UK) and were dissolved in water at 0.1 mg/mL.

The matrix used throughout these studies was 2,5-dihydroxybenzoic acid, dissolved in ethanol at 50 mg/mL. For the lactose sugars, 1 μL of sugar was applied to the probe tip and blown dry with warm air from an air gun. For the mannose-type sugars, 10 μL was applied to the probe tip. The sugars were then doped with 1 μL of 0.01 M NaCl to enhance the signal. Finally, 1 μl of matrix was applied to the probe tip. As noted by others,[34] all ions—even without doping—were the quasi-molecular sodium-adducted species, and all fragments are sodiated unless otherwise stated. No attempt was made to remove the sodium, which is ubiquitous in the sample and matrix.

RESULTS AND DISCUSSION

A series of milk sugars containing lacto-*N*-hexaose were studied. These compounds are all present in human milk or are the metabolites of sugars found in human milk.[35] The structure of difucosyllacto-*N*-hexaose (**I**) is given, and the MALDI/FTMS spectrum can be seen in Figure 2a. This spectrum has been previously published and is shown here again for comparison.[26] In Figure 2a, $[M + Na]^+$ is the predominant ion at *m/z* 1387.5, corresponding to the molecular weight of the neutral sugar plus a sodium atom. Fragmentation is also observed in Figure 2a. We classify this as "source fragmentation", because it is caused by the high energy of the laser and the extractor and repeller voltages used to extract the ions from the source. Whereas in MALDI-TOF it is important to work with a laser energy slightly above the laser irradiance threshold,[36] we have found this not to be the case in MALDI/FTMS. As calculated in the Experimental Section, the irradiance of our laser (1×10^7 W/cm^2) is higher than that commonly used in MALDI/TOF. It should be noted that MALDI spectra from magnetic sector instruments have also be obtained at high laser irradiance.[16] In our experience, it is less the laser irradiance and more the forming of the crystals that governs whether we obtain good signal.

The major source fragment observed in Figure 2a is at *m/z* 1241.4, corresponding to the loss of a fucose unit (loss of 146). The fucose glycosidic bond is very labile, contributing to nearly all the observed fragments of **I**. Using the nomenclature of Domon and Costello,[37] developed for the identification of oligosaccharide fragments in mass spectrometry, this is a Y_{3X}'' fragment. The designation X is used here to indicate that the fucosyl may be lost from either of the equivalent (α or β) antennas. The $Y_{3\alpha}''/Y_{3\beta}''$ fragment (*m/z* 1095.4) is also prominent, corresponding to the loss of both fucosyl units. The "/" is used to indicate multiple cleavages. Cross-ring cleavage products are observed at *m/z* 1327.5 and 1181.4, corresponding to fragmentation at the reducing end. Others have also shown that cross-ring cleavage occurs predominantly at the reducing end of the sugar.[38] This is because the simultaneous breaking of two bonds in a ring is less likely than a stepwise process, where the first step is the opening of the reducing ring. When the anomeric oxygen is protected, this ring-opening is hindered, and thus this fragmentation pathway is suppressed. Therefore, these fragments are assigned $^{0,2}A_4$ (*m/z* 1327.5) and $Y_{3X}''/^{0,2}A_4$ (*m/z* 1181.4). Loss of a complete antenna (Y_2) is observed at *m/z* 876.3, and a Y_2/Y_{3X}'' fragment is observed at *m/z* 730.2.

In all CID experiments, it is necessary to verify that fragments are originating only from the ion of interest. Figure 2b shows the isolation of the $[M + Na]^+$ ion by the ejection of all other ions in the ICR cell, as discussed in the Experimental Section.

Figure 2c shows the MS/MS spectrum of **I**. The CID excite event was 25 V_{b-p} for 0.25 ms, corresponding to a kinetic energy (E_{lab}) of 364.9 eV and an E_{com} of 7.22 eV. As mentioned previously, the E_{com} values are valid for the first collision only. Under these conditions, multiple collisions occur, and so E_{com} values are included for comparison only. Figure 2c clearly shows the extensive structural information that can be obtained in CID experiments, and Table 1 summarizes the fragments from Figure 2a and c. The dominant fragments in the MS/MS spectrum are the same as those resulting from the "source fragmentation". In addition, there are several fragments that are found only in the MS/MS spectrum. The fragment at *m/z* 1225.4 can correspond to either the loss of a galactose from the nonreducing end (Y_{3X}') or the loss of a glucose from the reducing end (C_3). Sugar units lost from the reducing end of an oligosaccharide are more likely to retain the glycosidic oxygen and thus result in B fragments. Therefore, it is likely that the *m/z* 1225.4 fragment is the Y_{3X}', the X again indicating that either of the two galactose units can be lost. A number of multiple generation peaks appear at *m/z* 1079.4 (Y_{3X}'/Y_{3X}''), 933.3 ($Y_{3\alpha}''/Y_{3\beta}''/Y_{3X}'$), and 714.2 ($Y_2/Y_{3X}'$). We assign *m/z* 1121.4 as a $Y_{3X}''/^{2,4}A_4$ fragment. Likewise, *m/z* 975.3 is assigned $Y_{3\alpha}''/Y_{3\beta}''/^{2,4}A_4$. We are aware that the $^{2,4}A_4$ fragment could also be assigned $^{0,2}X_3$, but again it is expected that the cross-ring cleavage occurs on the reducing end of the sugar. The fragment at *m/z* 1061.4 may be assigned Z_3'/Y_{3X}'' or B_3/Y_{3X}'' as well as the Y_{3X}'/Y_{3X}''-H_2O quoted in Table 1. Due to the lack of a fragment at *m/z* 1207.4 that would correspond to the Z_{3X}' or B_3 fragment alone, we feel that the assignment in Table 1 is correct. All other fragments in the MS/MS spectrum are combinations of the above mentioned fragments.

Figure 2c was obtained using a CID amplitude that maximized the number of fragments observed, yielding the optimum amount of structural information. To determine the dissociation threshold, CID experiments were repeated many times with the amplitude of the CID pulse varied each time, as discussed in the Experimental Section. The CID amplitude at which any fragmentation was first observed was found to be 16.6 V_{b-p}, and this is shown graphically in Figure 3. The only fragment ion at these CID conditions corresponded to the Y_{3X}'' cleavage, the loss of a fucose unit. This is somewhat expected, because in Figure 2a it was observed that the fucose glycosidic bond was very labile. A threshold of 16.6 V_{b-p} corresponds to 160.9 eV of kinetic energy and an E_{com} of 3.18 eV, using eqs 1 and 3, respectively. As mentioned in the Experimental Section, the error in the measure-

(34) Harvey, D. J. *Rapid Commun. Mass Spectrom.* **1993**, *7*, 614.
(35) Yamashita, K.; Tachibana, Y.; Kobato, A. *J. Biol. Chem.* **1977**, *252*, 5408.
(36) Ingendoh, A.; Karas, M.; Hillenkamp, F.; Giessmann, U. *Int. J. Mass Spectrom. Ion Processes* **1994**, *131*, 345.
(37) Domon, B.; Costello, C. E. *Glycoconjugate J.* **1988**, *5*, 397.
(38) Spengler, B.; Dolce, J. W.; Cotter, R. J. *Anal. Chem.* **1990**, *62*, 1731.

Chart 1

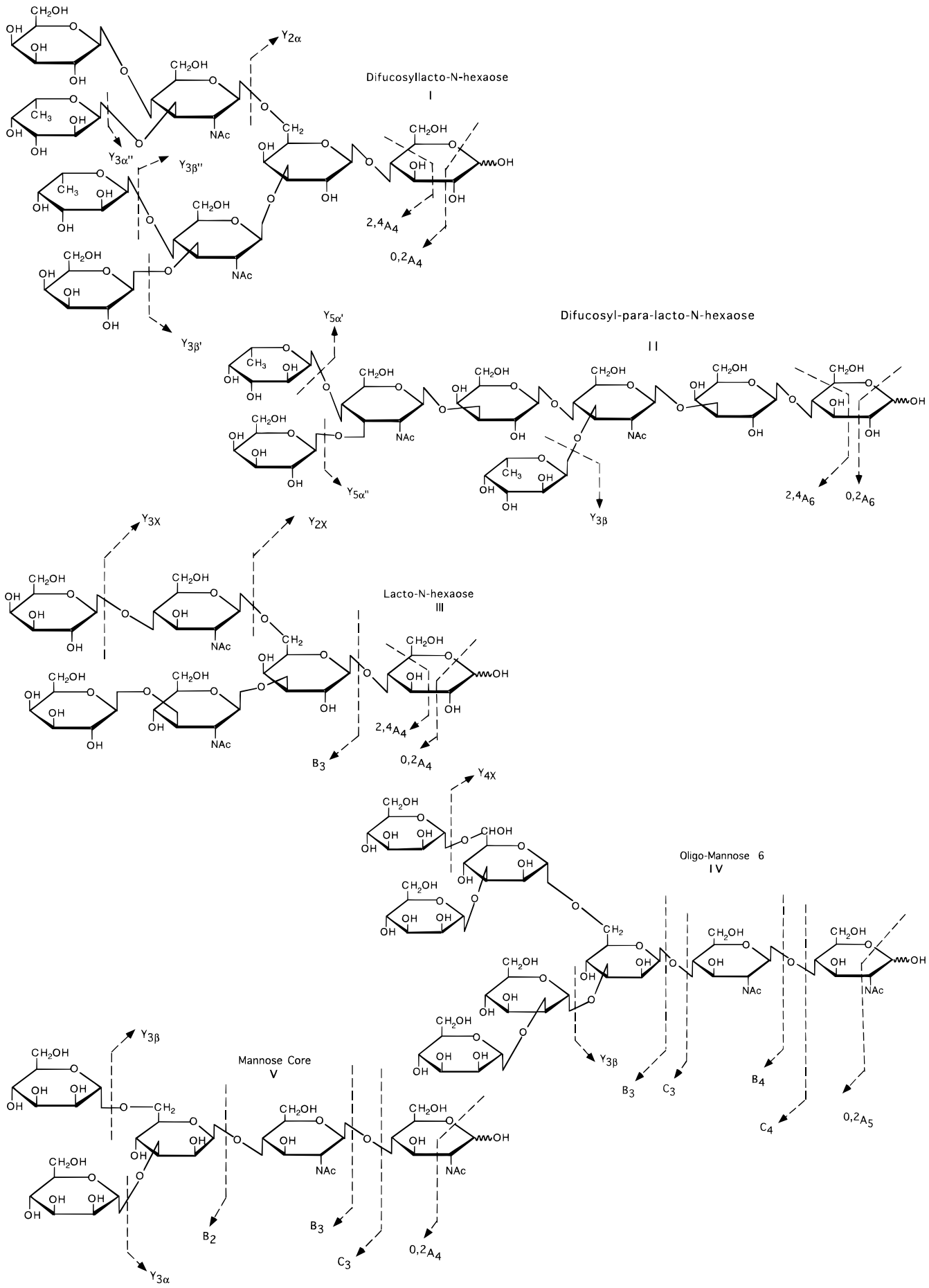
Difucosyllacto-N-hexaose
I
Difucosyl-para-lacto-N-hexaose
II
Lacto-N-hexaose
III
Oligo-Mannose 6
IV
Mannose Core
V

Table 1. Structural Assignments of the Peaks from MS and MS/MS of Difucosyllacto-*N*-hexaose (I) in Figure 2a and 2c[a]

m/z	fragment	MS	MS/MS
1327.5	$^{0,2}A_4$	+	+
1241.4	Y_{3X}''	+	+
1225.4	Y_{3X}' (1−3 or 1−4)	−	+
1181.4	$^{0,2}A_4/Y_{3X}''$	+	+
1121.4	$Y_{3X}''/^{2,4}A_4$	−	+
1095.4	$Y_{3\alpha}''/Y_{3\beta}''$	+	+
1079.4	Y_{3X}'/Y_{3X}''	−	+
1061.4	$Y_{3X}'/Y_{3X}''/-H_2O$	−	+
1035.3	$Y_{3\alpha}''/Y_{3\beta}''/^{0,2}A_4$	−	+
975.3	$Y_{3\alpha}''/Y_{3\beta}''/^{2,4}A_4$	−	+
933.3	$Y_{3\alpha}''/Y_{3\beta}''/Y_{3X}'$	−	+
915.3	$Y_{3\alpha}''/Y_{3\beta}''/Z_{3X}'$	−	+
876.3	Y_2	+	+
771.3	$Y_{3\alpha}''/Y_{3\beta}''/Y_{3\alpha}'/Y_\beta'$	−	+
730.2	Y_2/Y_{3X}''	+	+
714.2	Y_2/Y_{3X}'	−	+

[a] "+" indicates that the fragment was present in the spectrum, and "−" indicates that the fragment was not present. All other fragments are combinations of the above fragments.

ment of the onset of threshold may be ambiguous over a 0.5 V_{b-p} range, which corresponds to ±0.2 eV of center-of-mass frame energy. While we have nothing to compare these values to, they are of the same order of magnitude as values obtained for the CID of a similarly sized fullerene, C_{94}^+, using MALDI FTMS.[30] In **I** and in other fucose-containing sugars (results not shown), we always observe the loss of the fucose unit as a major fragment. While at present we do not have an explanation for this behavior, it is interesting to note that fucose is also labile in solution.[39] It is also the only L-sugar found commonly in nature.

It is known that doping oligosaccharides with alkali metals can increase the sensitivity and affect the fragmentation products.[9] In previous studies,[40] we have observed that the addition of different alkali metals to oligosaccharides can have a marked effect on the degree of fragmentation. The addition of Li^+ to large oligosaccharides is found to increase the amount of fragmentation, while Cs^+ minimizes it. This effect is caused by the size of the alkali metal ion, which in turn is related to the number of coordination sites the cation can possess. For cesium, at least five sugar subunits are needed in order to observe a $[M + Cs]^+$ during MALDI.[40] Molecular modeling has confirmed this effect, showing that the large cesium ion radius can interact with five sugar rings.[40] Therefore, if the sugar is large enough for cesium adduction to occur, fragmentation is dramatically reduced due to numerous Cs^+−O interactions, which stabilize the sugar/metal complex. For sodium, only disaccharides are needed for the observation of $[M + Na]^+$ species. But while the individual interactions are stronger for the smaller cations, the limited number of interactions do little to stabilize the oligosaccharide. Therefore, to quantify this effect in terms of kinetic energy and E_{com}, **I** was doped with CsCl, and once again the CID experiment was repeated multiple times at differing CID amplitudes to obtain dissociation thresholds. The first fragment to appear was still the Y_{3X}'' fragment, although now it was a cesium-adducted species.

(39) Lindberg, B.; Lonngren, J.; Svensson, S. *Adv. Carbohydr. Chem. Biochem.* **1975**, *31*, 185.

(40) Cancilla, M. T.; Penn, S. G.; Carroll, J. A.; Hedrick, J. L.; Lebrilla, C. B., submitted.

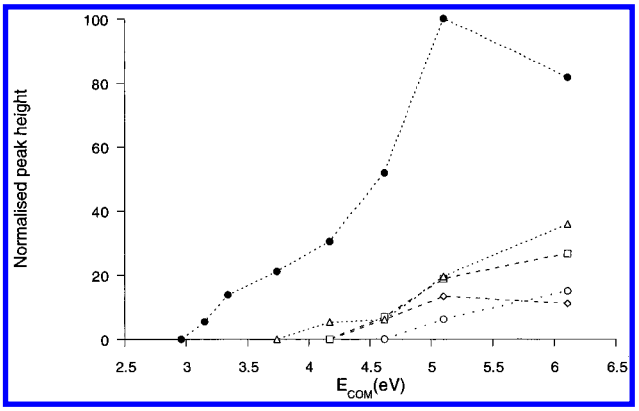

Figure 4. Plot of the appearance of fragmentation vs E_{com} for **II**: ◇, *m/z* 1327.5; ●, *m/z* 1241.4; □, *m/z* 1181.4; ○, *m/z* 1121.4; and △, *m/z* 1095.4.

Furthermore, the CID threshold had increased significantly to 19.5 V_{b-p}. This corresponds to 205.7 eV of kinetic energy and an E_{com} of 3.78 eV, and is significantly higher than that for the sodiated species (16.6 V_{b-p}; E_{lab} = 160.87 eV; E_{com} = 3.18 eV). The high dissociation threshold confirms that the cesium does stabilize the sugar, which is a general behavior of oligosaccharide/alkali metal complexes that has also been observed in FAB/FTMS.[41]

Although mass spectrometry is unable to directly differentiate between isomers, the use of fragmentation thresholds is an interesting approach to this problem. In previous work,[40] it has been found that fragmentation of oligosaccharides appeared to be a function of structure. Highly branched oligosaccharides tend to fragment less than linear structures under the same source conditions. The structural isomer of **I**, difucosyl-para-lacto-*N*-hexaose (**II**), was investigated to see if fragmentation threshold varied with structure. Compound **II** has a more linear structure, whereas **I** is more branched. For the mass spectrum of **II** (not shown), overall fragmentation increased compared to that for **I**, as expected due to the more linear structure.[40] Once more, the fragmentation threshold was measured by repeating the CID experiment at a number of differing CID voltages. Again, the first fragment to appear at lowest energy was due to the loss of a fucose unit, the $Y_{5\alpha}''$ or $Y_{3\beta}$. It was found that the dissociation threshold for the loss of a fucose was 16.5 V_{b-p}. Thus, the losses of fucose from both sodiated isomers **I** and **II** require the same energy, within experimental error. The similarity of the results will certainly be because the same cleavage reaction is occurring, and this effect masks other differences that may be due to structure. If different fragmentation thresholds can be found for sugar types other than fucose, this may be an approach to distinguishing between, for example, glucose and galactose, where the masses are identical and only bond orientation differs.

Figure 4 shows a plot of CID amplitude against normalized fragment peak height not only for the $Y_{5\alpha}''$ or $Y_{3\beta}$ fragment but also for a number of other structurally significant fragments of **II**. Table 2 also shows the dissociation thresholds for these fragments. To observe the $Y_{5\alpha}''/Y_{3\beta}$ fragment (loss of both fucose) of **II** requires a minimum CID excite voltage of 19 V_{b-p} (4.17 eV E_{com}). This relatively high value is expected since two distinct moieties are lost. We are, at present, assuming that the fucose units are equivalent, even though one is a 1−3 linkage and the other is a 1−4 linkage. A cross-ring cleavage ($^{0,2}A_6$) occurs at 20

(41) Ngoka, L. C.; Gal, J. F.; Lebrilla, C. B. *Anal. Chem.* **1994**, *66*, 692.

Table 2. CID Energies for the Fragments of Difucosyl-para-lacto-*N*-hexaose (II) in Figure 4

m/z	type of fragment	CID pulse (V_{b-p})	E_{com} (eV)
1327.5	cross-ring cleavage, $^{0,2}A_6$	20.0	4.62
1241.4	glycosidic bond breakage (loss of fucose), $Y_{3\beta \text{ or } Y5\alpha}''$	16.5	3.15
1181.4	$^{0,2}A_6/Y_{3\beta}$ or $^{0,2}A_6/Y_{5\alpha}''$	20.0	4.62
1121.4	$^{2,4}A_6/Y_{3\beta}$ or $^{2,4}A_6/Y_{5\alpha}''$	21.0	5.10
1095.4	$Y_{3\beta}/Y_{5\alpha}''$	19.0	4.17

V_{b-p} (4.62 eV E_{com}), suggesting that this is a higher energy process than the glycosidic bond cleavage. The $^{0,2}A_6/Y_{5\alpha}''$ or $^{0,2}A_6/Y_{3\beta}$ fragment also appears at 20 V_{b-p} (4.62 eV E_{com}), as this is the loss of a fucose *and* a cross-ring cleavage. At 21 V_{b-p} (5.10 eV E_{com}) a further fragment corresponding to the loss of 120 from the parent appears. Again, we are unable to unequivocally discriminate between $^{2,4}A_6$ and $^{0,2}X_5$, but for reasons given previously we assume that fragmentation occurs at the reducing end of the sugar, hence giving a $^{2,4}A_6$ fragment. It is likely that the $^{2,4}A$ fragment originates from the $^{0,2}A$ fragment, as the $^{2,4}A$ fragment occurs at a higher energy (21 V_{b-p}) than the $^{0,2}A$ fragment (19 V_{b-p}). The remainder of the fragments in the MS/MS spectrum are combinations of the above fragments. At CID bursts above 25 V, we lose signal, presumably because the cyclotron radius is larger than the ICR cell dimensions. The cyclotron radius of **II** at 25 V_{b-p} is calculated to be 3.2 cm, versus 2.5 cm for the radius of the cell. The dissociation thresholds for the above mentioned fragments of **II** were also compared to the dissociation thresholds of the corresponding fragments of **I**. We have already seen that the dissociation thresholds for the loss of the fucose from both **I** and **II** were similar. This was found to also be true for other fragments, namely the cross-ring cleavage ($^{0,2}A_x$) and the cross-ring cleavage + loss of fucose fragment ($^{0,2}A_x/Y_x$). Once again, the similarity of the results is due to the same cleavage reaction occurring, masking any subtle structural effects.

Figure 5a shows the mass spectrum of lacto-*N*-hexaose (**III**). This is the core compound for a number of sugars found in human milk (e.g., **I** and **II**). Figure 5b shows the MS/MS, where the CID amplitude was 18 V_{b-p} for 0.25 ms. Table 3 shows the assignments of the fragments. While the CID experiment certainly enhances the "source" fragmentation, only one additional fragment is observed at *m/z* 610.2. This compound appears to be very resistant to fragmentation, and this phenomenon has been observed with another core compound, mannose core (**V**). To gain further information, MS^n, where $n > 2$, would need to be attempted, and this is discussed later. The asterisks indicate noise spikes at *m/z* 770.7 and 652.5.

A number of *N*-linked oligosaccharides were also studied: oligomannose 6 (**IV**) and mannose core (**V**). The mass spectrum of **IV** is given in Figure 6a and the CID spectrum in Figure 6b, and mass assignments are given in Table 4. Briefly, the dominant fragment in both the MS and the MS/MS is the loss of the terminal *N*-acetylglucosamine (GlcNAc) residue, giving an ion at *m/z* 1198.4 (B_4). Other fragments present in the MS and further enhanced in the MS/MS are the fragments at *m/z* 995.3 (B_3), 1013.3 (C_3), 1036.3 (B_4/Y_{4X}), 1216.4 (C_4), 1257.4 (Y_{4X}), and 1318.4 ($^{0,2}A_5$). There are two new fragments in the CID spectrum at *m/z* 833.2 (B_3/Y_{4X}) and 874.3 ($B_4/Y_{3\beta}$). It should be noted that *m/z* 874.3 could also be a $B_4/Y_{4X}'/Y_{4X}''$. Without further MS experiments, we cannot say whether the mannose units are lost

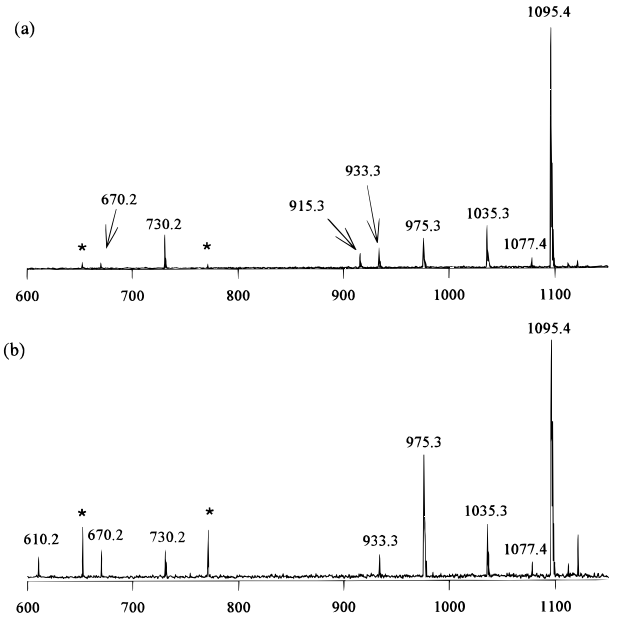

Figure 5. (a) Mass spectrum of lacto-*N*-hexaose (**III**). (b) MS/MS of **III**, excited to 5.98 eV E_{com}.

Table 3. Structural Assignments of the Peaks from MS and MS/MS of Lacto-*N*-hexaose (III) in Figure 5

m/z	fragment	MS (Figure 5a)	MS/MS (Figure 5b)
1077.4	$-H_2O$	+	+
1035.3	$^{0,2}A_4$	+	+
975.3	$^{2,4}A_4$	+	+
933.3	Y_{3X}	+	+
915.3	B_3	+	−
730.2	Y_{2X}	+	+
670.2	$Y_{2X}/^{0,2}A_4$	+	+
610.2	$Y_{2X}/^{2,4}A_4$	−	+

[a] "+" indicates that the fragment was present in the spectrum, and "−" indicates that the fragment was not present.

separately, as in the Y_{4X} fragments, or as a discreet unit, as in the $Y_{3\beta}$ fragment. But using the previously given theory that linear molecules tend to fragment more than branched ones, we may postulate that the $B_4/Y_{4X}'/Y_{4X}''$ fragment will lead to a molecule containing more branching points and so may be more favorable. While these new fragments in the MS/MS spectrum are combinations of those already present in Figure 6a, they do give extra information as to the sequence of the sugar subunits not deducible from Figure 6a. MS/MS of the *m/z* 1198.4 fragment would also yield more information. The ratios of the peak heights of *m/z* 1198.4 and 216.4 in Figure 6 show clearly how, when cleavage occurs from the reducing end, B fragmentation (*m/z* 1198.4) is much more favorable than C fragmentation (*m/z* 1216.4). The inset to Figure 6a also shows that unit mass resolution is obtained for these spectra. In general, unit mass resolution is obtained in all spectra. The broadness of the peaks is an artifact due to the transfer of individual points to a spreadsheet program for insertion into this document.

All *N*-linked oligosaccharides, including **IV**, contain a common pentasaccharide core consisting of three mannose and two GlcNac residues, called the mannose core (**V**). The mass spectrum of **V** is shown in Figure 7a. The dominant ion is the pseudomolecular $[M + Na]^+$ (*m/z* 933.3), and a peak corresponding to the potassiated species is also observed (*m/z* 949.2). The large

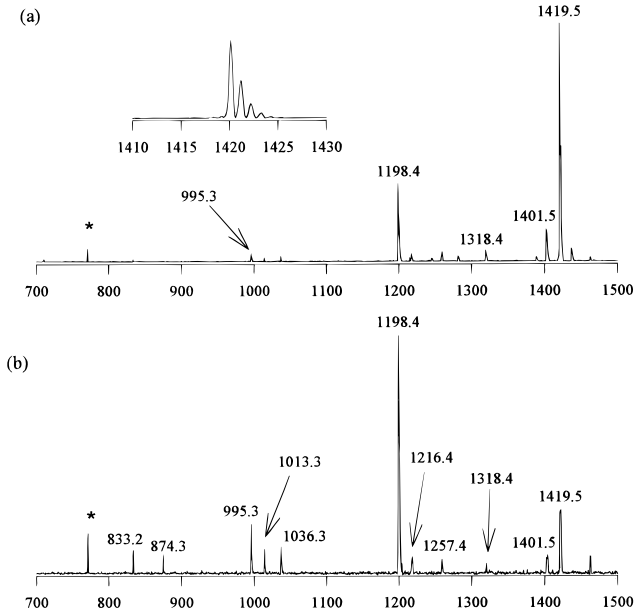

Figure 6. (a) Mass spectrum of oligomannose 6 (**IV**). (b) MS/MS of **IV**, excited to 5.84 eV E_{com}.

Table 4. Structural Assignments of the Fragmentation of Peaks of Oligomannose 6 (IV) in Figure 6

m/z	fragment	*m/z*	fragment
1401.5	$-H_2O$	1036.3	B_4/Y_{4X}
1318.4	$^{0,2}A_5$	1013.3	C_3
1257.4	Y_{4X}	995.3	B_3
1216.4	C_4	874.3	$B_4/Y_{3\beta}$
1198.4	B_4	833.2	B_3/Y_{4X}

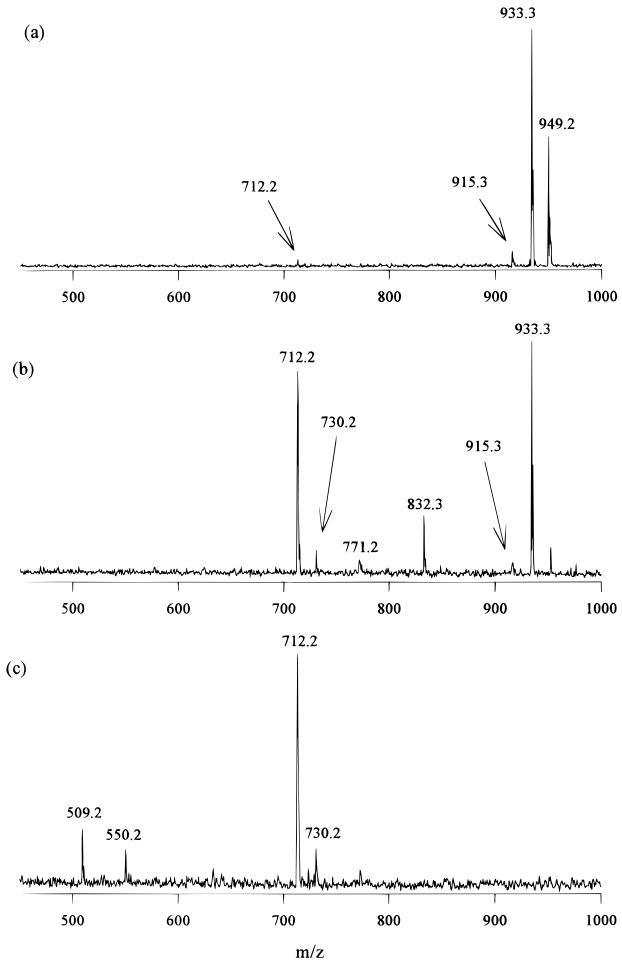

Figure 7. (a) Mass spectrum of mannose core (**V**). (b) MS/MS of **V**, excited to 7.31 eV E_{com}. (c) MS/MS/MS of the B_3 fragment of **V**, excited to 6.20 eV E_{com}.

potassium species is present because the solutions were stored in glass. Little fragmentation of the mannose core is observed, with a peak due to the loss of water (*m/z* 915.3) and a B_3 (*m/z* 712.2) fragment due to the loss of GlcNAc. The lack of fragmentation is expected due to the degree of branching in comparison to the small size of the molecule.[40] From a biological point of view, this may be significant, because this pentasaccharide is present in all N-linked oligosaccharides, and its inherent stability may be the reason it is used to link the carbohydrate portion of N-linked glycoproteins. It is interesting to note that lacto-*N*-hexaose (**III**), the other core sugar studied, was also relatively resistant to fragmentation.

It is examples like Figure 7a that show MS/MS to be a very powerful technique. Because of the limited "source" fragmentation, MS/MS was carried out on the $[M + Na]^+$ ion using a CID amplitude of 17 V_{b-p} for 0.25 ms (Figure 7b). The MS/MS spectrum shows that the major fragment is still the loss of GlcNAc (B_3, *m/z* 712.2), but there are also additional fragments. A C_3 fragment is present at *m/z* 730.2, and an $^{02}A_4$ cross-ring cleavage (*m/z* 832.3). A mannose moiety is lost to give a fragment at *m/z* 771.2 (Y_{3X}). At this time we are unable to deduce whether it is the 1−6 ($Y_{3\beta}$)- or the 1−3 ($Y_{3\alpha}$)-linked sugar that cleaves.

The fragmentation observed in the MS/MS spectrum was still limited, and so, to obtain even more structural information, MS/MS/MS was carried out (Figure 7c) by isolating the B_3 ion from the MS/MS spectrum shown in Figure 7b. In the MS/MS/MS spectrum (Figure 7c), more additional fragments are observed at *m/z* 550.2 ($Y_{3\alpha}/B_3$) and 509.2 (B_2). The C_3 (*m/z* 730.2) peak is still present, as this was not completely removed during the second isolation process. Nonetheless, it can be clearly seen that each additional MS experiment leads to further structural information, and with good signal-to-noise, and that these techniques are especially powerful for molecules that fragment little during ionization. Further work is under way to attempt MS^4 with the same ease and for larger oligosaccharides. Experiments of this type are crucial to the detailed analysis of the structure of complex oligosaccharides, as the above examples demonstrate.

CONCLUSIONS

We have successfully carried out MS, MS/MS, and MS/MS/MS of MALDI-generated oligosaccharide ions by external source FTMS. To our knowledge, this is the first account of the CID of MALDI-generated ions by external source FTMS to appear in the literature. For the sodiated isomers of difucosyllacto-*N*-hexaose (**I**), MS/MS gives extensive fragmentation, leading to detailed structural information. Using dissociation thresholds, it was found that the loss of the fucose sugar, a major fragment, has the lowest barrier to fragmentation. When the oligosaccharide is complexed to cesium, the dissociation threshold is considerably increased, indicating that coordination between the metal and the sugar stabilizes the complex. The dissociation thresholds for other fragments show that glycosidic bond cleavage occurs at a lower CID energy than cross-ring cleavage.

Multiple CID experiments were carried out on mannose core (**V**), and each level of experiment gave more structural information

than the "source" fragmentation. MS/MS/MS gave addition information, with only small loss in signal. Experiments of this type are currently being applied to other biologically important unknown sugars. These results demonstrate the utility of the method in the determination of unknown oligosaccharide structures.

ACKNOWLEDGMENT

The authors thank Dr. Jerry L. Hedrick for the kind gift of the mannose-type sugars and for many helpful discussions. Funds provided by the National Institute of General Medical Sciences, NIH (GM49077-01), are gratefully acknowledged.

Received for review February 16, 1996. Accepted April 30, 1996.[⊗]

AC960155I

[⊗] Abstract published in *Advance ACS Abstracts,* June 15, 1996.